Published in final edited form as:
Retina. 2009 ; 29(7): 1002–1012. doi:10.1097/IAE.0b013e3181a0be05.

Molecular Karyotype of Sporadic Unilateral Retinoblastoma Tumors

Arupa Ganguly[1], **Kim E. Nichols**[2], **Gregory Grant**[3], **Eric Rappaport**[4], and **Carol Shields**[5]

[1] Department of Genetics, University of Pennsylvania

[2] Division of Oncology, Children's Hospital of Philadelphia

[3] Department of Bioinformatics, University of Pennsylvania

[4] NAPCORE, Children's Hospital of Philadelphia

[5] Ocular Oncology Service, Wills Eye Institute, Philadelphia, PA

Abstract

Background—Retinoblastoma (RB) is a childhood ocular malignancy associated with mutations in *RB1*, a tumor susceptibility gene. Inactivation of both copies of the *RB1* gene in a retinal cell is followed by the sequential acquisition of additional genetic changes that define the course to tumor formation.

Methods—To identify the genetic events that cooperate with loss of the *RB1* gene function, we performed a whole genome sampling assay (WGSA) based on SNP genotyping. We used DNA isolated from 25 sporadic, unilateral RB tumors and matched blood samples.

Results—Genomic profiles were analyzed to identify regions of loss of heterozygosity (LOH) and/or amplification. Two major subclasses of RB tumors were defined by the presence (n=18) or absence (n=7) of LOH of chromosome 13. LOH in most cases was due to copy neutral events caused by mitotic recombination and mitotic non-disjunction. Tumors harbored novel regions of amplification at 1q44, 3p25, 11q14, 11q25, 14q23, 15q21, 16p13, 17p11.2, 19q13, and 20q13 while regions of loss included 6q22, 7q21and 21q2.

Conclusion—WGSA-based analysis of unilateral RB tumors revealed novel regions as significant. These minimum critical regions that are lost or amplified are expected to harbor genes that aid the process of tumorigenesis.

Keywords

Molecular Karyotype; Retinoblastoma; SNP-array; Whole Genome Sampling Assay

Introduction

Retinoblastoma (RB) is a tumor of the eye that occurs in children and can lead to compromised vision or possibly death if not diagnosed and treated properly. RB is associated with mutations in *RB1*, a tumor susceptibility gene [1]. Cell cycle exit and terminal differentiation of retinal cells are serial events that ensure proper retinal development [2]. The *RB1* gene encodes pRB, a nuclear protein that plays a critical role in this regulated series of events. RB tumors represent

Corresponding Author: Arupa Ganguly, PhD, Department of Genetics, University of Pennsylvania, Philadelphia, PA 19104.
There is no conflict of interest for any one of the authors.

a deregulation of this process. Inactivation of both copies of the *RB1* gene in a retinal cell, through mutations or epigenetic modifications, initiates the onset of RB. This event is followed, as in other cancers, by the sequential acquisition of additional genetic abnormalities that define the course leading to tumor formation and metastasis [3–8].

Genomic instability contributes to the progression of retinoma to malignant retinoblastoma [9–11]. In humans, this progression is characterized by loss of both copies of the *RB1* gene in retinoma, followed by changes in the copy number of oncogenes such as *MYCN* (2p24.3), *E2F3* and *DEK* (6p22), *KLF14* (7q32) and *MDM4* (1q32), as well as tumor suppressor genes *CDH11* (16q21) and $p75^{NTR}$ (17q21). It has also been shown that when *RB1* and *TP53* are inactivated in mice, retinoblastoma develops [12,13]. Similarly, inactivation of *RB1* and *RBL1* (p107) or *RB1* and *RBL2* (p130) give rise to retinoblastoma in mice, where *RBL1* and *RBL2* are members of the *RB1* gene family with redundant but unique functions [14–16]. Collectively, these observations indicate that, beyond biallelic inactivation of *RB1*, a third and additional “hits” are required for the development of RB tumors in humans and mice [13,17–19].

Comparative Genomic Hybridization (CGH) is an analytical tool used to identify regions of chromosomal loss and gain within tumors by comparing pooled normal DNA with tumor DNA. Several studies have used CGH to characterize genomic abnormalities in RB tumors [20–31]. Previously identified recurrent abnormalities include gain of chromosomal material at 6p, 1q, 2p, 13q and 19 and loss of material on chromosome16, 16q and 13q. Each of these abnormalities was observed in at least 10% of tumors studied in more than one series [20–22]. The gain of 6p, as in isochromosome 6p, was particularly common and seen in 44% to 69% of tumors. Some abnormalities, such as gain of 6p or 13q and loss of 13q, were more common in tumors with high-risk histological features; however, only the association with loss of 13q was statistically significant [20]. In three patients who developed extra-ocular relapse, tumors showed loss of 13q and two out of three also had loss of 5q, suggesting that loss of genetic material at these loci may be associated with metastasis [32]. Older children (> 36 months of age at enucleation) tend to have more CGH abnormalities per tumor than younger children (<12 months; median numbers 11 vs. 3). In addition, +1q, +13q, −16, and −16q were more frequent in children with an older age at enucleation. Recently it has been shown that loss or retention of specific regions of 1q correlated with the degree of differentiation of RB tumors [33].

Therefore, it is clear that identification of these genomic alterations serve as clues to better understand the molecular basis of RB tumor formation, and could pave the way to novel and more directed therapies.

In this report, we describe the molecular karyotype of 25 sporadic unilateral RB tumors as determined by the use of a whole genome sampling assay (WGSA), which incorporated the SNP genotyping of matched normal and tumor tissue. The WGSA method involves parallel genotyping of many bi-allelic single nucleotide polymorphisms located across all 23 chromosomes of the human genome. Comparison of the genotype calls and intensities of the different alleles from matched normal and tumor tissue samples allows one to determine regions of loss of heterozygosity or amplification in the tumor with high resolution.

Methods

Unilateral RB tumor specimens (italics, like other sections)

Primary unilateral RB tumors were collected at the Genetic Diagnostic Laboratory, University of Pennsylvania, and at Wills Eye Institute. For inclusion in this study, the tumors could not have received any therapy before enucleation. The protocol for genetic analysis of tumors was

approved by the IRB of the University of Pennsylvania (Protocol number 706577, original approval date 09/23/05). Tumor samples were flash frozen and transferred on dry ice. Blood samples from affected individuals were collected in EDTA-containing tubes and transferred at room temperature.

Isolation of DNA from blood and frozen tumor samples

Genomic DNA was isolated from 1 to 3 ml of blood and frozen tumors using a commercial DNA isolation kit (Gentra, CA) following the manufacturer's instructions.

Whole Genome Sampling Assay (WGSA)

The data for this report was generated using the 10K Single Nucleotide Polymorphism (SNP) chips from Affymetrix, CA. These Chips provided a platform for the parallel query of 10,000 SNPs selected from the human genome that are gene-centered and located within 10KB of the flanking sequences of any gene. The average distance between SNPs is 250KB and the average rate of heterozygosity is 0.37. A single array analysis was performed for each DNA sample (250 ng each) using the protocol defined by the manufacturer. In brief, DNA samples were digested with Xba1, ligated to an adaptor and amplified using a set of universal primers (available as components of Assay Kits P/N 900520 and 900521). The amplified DNA was fragmented, labeled with a fluorescent dye and hybridized to a chip. Hybridization and post hybridization washes were done in the Affymetrix fluidics station followed by scanning and analysis.

Data Analysis

Affymetrix GeneChip DNA Analysis Software (GTYPE V3.0), was used to perform automatic base calls with high base-calling accuracy, reproducibility and automatic generation of SNP summary reports [34]. The output data from GTYPE was analyzed using dCHIPSNP (http://www.biostat.harvard.edu/complab/dchip/snp/), a program that allows visualization of regions of loss or gain along the length of a chromosome [35,36]. A "call" for a region of loss or gain is based on compiled data for at least 10 consecutive SNPs genotyped within a chromosomal region spanning 10 MB. The genome build of July 2003 human reference sequence (NCBI Build 34) was used for defining genomic regions.

Significance Testing for Aberrant Copy-number (STAC)

The output from the dCHIPSNP analysis offers a simple multi-sample p-value for LOH, which tests the null hypothesis that there is no aberration at a given location in any of the samples. Once the significant aberrations are identified, it is important to define concordant aberrations across multiple samples. To address this need, we used an algorithm called STAC (Significance Testing for Aberrant Copy-number) (www.cbil.upenn.edu/STAC) [37], which defines two statistics, frequency (f) and foot-print (fp) to measure concordance across multiple samples. For each statistic and each location a multiple testing corrected permutation p-value is computed under a null permutation distribution. Frequency measures the number of aberrations present at a specific chromosomal location across samples. Footprint measures tightness of alignment of a set of aberration intervals that cover a given location [37].

Results

Sporadic unilateral RB occurs in a child without any family history, affects only one eye and has a later age of onset (average 2.5 years) compared to bilateral disease (average <1 year). It is caused by post-zygotic, somatic mutations of the *RB1* gene in a retinal progenitor cell. However, in 10% of sporadic unilateral RB, a germline mutation is present. The latter class of mutations is generally associated with 'low penetrance' in that they are predicted to have subtle

effects on the function or relative amounts of the expressed pRB protein. In addition mosaicism, germline or somatic, for de novo mutations have also been observed for unilateral RB.

The 25 sporadic unilateral RB samples included in this report were collected as part of a limited study for genetic testing of the mutation spectrum at the *RB1* locus of unilateral tumors. However, the clinical information on the RB tumors was not collected as part of this study and is thus unavailable for comparison with genomic profile. There were 17 females and 8 males with ages of onset ranging from 0.3 years to 7.4 years. Using complementary assays, we were able to identify inactivating bialelic *RB1* gene mutations in 100% of these tumors (Table 1). Of the 15 point mutations detected, 5 were C>T transitions in CpG dinucleotides. These data are consistent with prior studies demonstrating that methylation at cytosines within CpG islands generates hot spots for mutation in the *RB1* gene. Among the tumor-associated mutations identified, 10 out of 15 (67%) were protein-truncating mutations. We also observed methylation of the promoter region as the mode of *RB1* gene inactivation in 7 out of 25 (28%) tumors analyzed.

WGSA for determination of copy number variation

We used Affymetrix 10K SNP chip-based WGSA to generate genomic profiles of loss and/or gain of chromosomal material in unilateral RB tumors. The SNP call rates for DNA isolated from peripheral blood ranged between 89% and 99% while that for DNA isolated from tumor samples ranged between 86% and 99%. In all cases, the SNP calls from peripheral blood DNA were considered the "normal" standards, against which the SNP calls from tumor-derived DNA were compared. Loss of heterozygosity (LOH) or retention of heterozygosity (ROH) in the tumor was determined by comparing the blood and tumor SNP genotype calls.

Figure 1 demonstrates the output from the dCHIPSNP analysis as a whole genome LOH profile for the set of 25 paired normal/tumor samples (each indicated as separate columns). The summarized data indicate the LOH profile for each individual chromosome (indicated by the respective numbers on the left). The regions marked in yellow indicate retention of heterozygosity (ROH) and blue indicates regions of LOH. The clustering indicated on the top is obtained based on the co-occurrence of regions of loss in the tumors. The distances are based on the extent of discordance between the regions of 'significant' LOH between the individual tumors. The classification is unsupervised and can lead to unbiased schemes of identification of the sub-classes of tumors.

One of the advantages of WGSA is its ability to simultaneously derive SNP genotype as well as the relative copy number of each SNP based on information gained from the signal intensity of hybridized DNA. The upper panel in Figure 2A indicates the LOH profiles for chromosome 13 for direct comparison with the copy number profiles, which are shown in the lower panel. For copy number, the shades indicate values ranging from 0 (white) to ≥ 6 (dark red). More than half of the RB tumors had loss of heterozygosity at 13q (indicated by blue regions on the upper panel), the most common form of inactivation of *RB1*. Three tumors (710T, 443T and 044T) exhibited homozygous loss of the region encompassing *RB1* (indicated by white regions and the arrows). For two tumors, 610T and 710T, the LOH region (<250 kb) was small and below the level of detection using the 10K SNP chips, where the average distance between consecutive SNPs is approximately 250 KB.

Aberrations on other chromosomes

Figure 2B shows the copy number profiles for chromosomes 1 and 6. We observe that amplifications of chromosome 1q and 6p are highly correlated– in 12 out of 14 tumors with 1q amplification (86 %), we also found amplification of 6p. Fifteen out of 25 tumors exhibited

amplification of almost the entire 6p arm (60%). These data most likely reflect the tumors with isochromosome 6p, a very common aberration seen in RB tumors.

Figure 3 shows the clustering of the RB tumors based on copy number aberration (CNA) as opposed to LOH as in Figure 1. The cluster on the left includes 3 tumors, 912T, 913T and 620T, with the least number of aberrations and the cluster on the right includes 7 tumors with aberrations along the entire genome. The cluster in the middle includes tumors with specific aberrations: one subset with amplification of 1q, one subset with 6p amplification and a third subset with co-amplification of 1q and 6p.

Significance Testing for Aberrant Copy-number (STAC)

We applied STAC to the copy number output from dCHIPSNP on the cohort of 25 pairs of normal/tumor DNA samples to identify statistically significant regions of concurrent amplification/loss. Figure 4 shows the STAC output for the shared regions of gain or loss along the lengths of individual chromosomes (Table 2). The regions indicating gain (green bars) or loss (red bars) across the whole genome are those with the most significant changes in copy number (p values 0.05). STAC is designed to localize regions of concurrent aberration across multiple samples, within a chromosome arm, down to 1Mb resolution or less. Therefore, if an entire chromosome is gained or lost across all, or most samples, STAC will generally not give a significant p-value. This is the case for chromosome 6p, where the entire arm is amplified in 60% of the tumors. Such gross aberrations are easily identified by other means. STAC is designed to highlight the concordant local aberrations, and to distinguish them from the aberrations unique to a single sample.

Using STAC, we identified several recurrent regions of amplification or loss that are in agreement with previous studies. For example, STAC correctly identified 2p24.3 as an amplified region that harbors the *MYCN* gene, a known region of amplification in RB tumors. The complete list of chromosomal regions amplified or lost with p-values smaller than 0.05 is included in Table 2. In addition to previously identified regions, we also observed that there were several novel loci exhibiting gain or loss. These novel chromosomal regions are indicated by the asterisk next to the cytoband and include amplifications at 1q44, 3p25, 11q14 and 11q25, 14q23, 15q21, 16p13, 17p11.2, 19q13, and 20q13.33. Novel regions of loss included 6q22, 7q21and 21q2.

Gains along chromosomes 1q and 14q as revealed by significant fp-value (Table 2) are shown in Figures 5A and 5B. There are three regions of significant gain on chromosome 1 with the shade of grey indicating the level of significance. Thus the region between nucleotides 200, 000, 001 – 206,000,001 (chromosome 1q32.1–32.3) has significant regions of gain with sub-regions of highly significant gain (p-value less than 0.019; adjusted for multiple testing). Similarly, the significance of gain in the region on 1q44 is 0.0099 and includes *SMYD3*, a histone methyltransferase that plays a role in transcriptional regulation as a member of an RNA polymerase complex. While chromosome 1q gains are known, gain on 14q22.3 –23.1 is novel. One of the regions resides on chromosome14q23.1–23.3 and includes the gene encoding CEP170, a protein involved in centriole architecture, which when deregulated gives rise to chromosomal non-disjunction during mitosis.

Discussion

This report describes the molecular karyotype of primary unilateral RB tumors as determined by use of a SNP-array based WGSA on matched DNA samples from normal and tumor tissue. This study is limited to unilateral RB tumors as bilateral RB tumors are usually not enucleated before therapy. The aim of this project was to identify minimal critical genomic regions that are gained or lost in multiple samples of primary RB. The advantages of the SNP array based

genomic approaches include confirmation of previously reported chromosomal gains/losses, detection of copy neutral LOH and higher resolution mapping of novel genomic regions of loss or gain leading to the identification of target oncogenes and tumor suppressor genes.

The results included in Figure 1 indicate that LOH on chromosome 13 is the major genetic alteration driving the clustering of RB tumors. Excluding losses on chromosomes 6 and 16, there are only infrequent regions of LOH or homozygous loss across the genome of RB tumors. Upon closer inspection in Figure 2, two different classes of RB tumors are identified, including those with and without LOH for chromosome 13. The lower panel indicates the CNA output for the same set of paired samples. It is evident that for the right cluster of tumors with LOH (top panel), the copy number data does not indicate any loss of genetic material (lower panel). This finding supports the known concept that *RB1* inactivation leads to mitotic non-disjunction and LOH due to duplication of the mutant allele [38]. For 7 out of 16 tumors with LOH around the *RB1* gene locus, there is amplification of the retained allele (as indicated by the darker red color in 014, 902, 840 and 142), which may represent double strand breaks during DNA replication followed by aberrant DNA repair. There is also a subclass of RB tumors where the LOH/aberrations are limited to segments of chromosome 13. In these cases, mitotic recombination rather than non-disjunction, likely explains the development of LOH. Therefore, these events reflect aberrant sister-chromatid exchange and compromised double strand break repair machinery. Both of these modes of copy-neutral LOH attest to the known properties of pRB protein in maintaining genomic stability.

STAC is designed to localize regions of concurrent aberration across multiple samples, within a chromosome arm, down to less than 1Mb resolution [37]. Using this method, we found that the recurrent regions of amplification or loss, as indicated in Figure 4, include all regions identified in previous studies and as well as 13 novel chromosomal regions (indicated by the asterisk next to the cytoband) [7,33,39,40]. For example, one of well-established hallmarks of RB tumors is the presence of *MYCN* amplification (Reference). Indeed, we observed this event in 15 out of 25 tumors (60%) (Figures 3 and 4; Table 2).

The novel regions of amplification or loss with highest level of significance are indicated in bold letters in Table 2. We confirmed the validity of these regions by repeating WGSA using 250K SNP chips and reproducing the same results (data not shown). The novel regions amplified included 1q44, 3p25, 11q14 and 11q25, 14q23, 15q21, 16p13, 17p11.2, 19q13, and 20q13.33. The regions of significant loss included 6q22, 7q21and 21q2. The total number of genes in these chromosomal regions is large due to the limited resolution of the SNP-chip platform used in this report. The use of higher resolution platforms is expected to further narrow these minimum regions of chromosomal aberration.

Copy number variations have been detected as a natural variation of human genomic DNA [41,42]. Some of the identified regions of amplification or deletion in Table 2 overlap previously identified copy number polymorphism regions. However the data for this report has been generated using matched DNA from normal and tumor tissue. Therefore, only copy number changes that are different between normal and tumor tissue are detected as significant.

Gains along chromosomes 1q and 14q as revealed by significant fp-value (Table 2) are shown in Figure 5. Figure 5A demonstrates gains on chromosome 1. It has been established that mouse models of RB require inactivation of *TP53* in addition to *RB1*. Mutations in *TP53* gene were not detected in this set of RB tumors (data not shown) and these results confirm what is known in the literature [43]. However amplification of *MDM4* has been observed as an alternate pathway for inactivation of *TP53* in the mouse model. Consistent with this model, in our dataset, the amplified region of 1q32 includes *MDM4, GAC1,* and others, which encode proteins involved in the TP53 pathway and regulate p53 activity [43].

Figure 5B demonstrate gains on chromosome 14. While chromosome 1q gains are known, significant gain on 14q23.1–23.2 is novel. The list of genes present in 14q23.1 includes *CEP170* and *SIX1* and *SIX4* (genes associated with bilateral anophthalmia). The clustering of the RB tumors based on CNA (Figure 3) identifies tumors with different degrees of genomic instability. It is known that tumors from younger children have fewer numbers of aberrations [22]. Tumors 913T, 912T and 620T have the least number of aberrations genome wide and belong to children ages 0.4y, 0.3y, and 1 y respectively. In contrast, the 7 tumors belonging to the cluster on the extreme right with the most aberrations are derived from older children age 7.4y, 3.2y, 2.5y, 3.2y, 2.6y, 4.5y and 0.7y(the only exception) respectively (last column, Table 2). The tumors in the middle have co-amplifications of chromosome 1q and 6p.

In conclusion, the use of WGSA to examine unilateral RB tumors revealed novel features of the genomic architecture. The major advantage of the SNP based analysis was the identification of regions of copy neutral LOH. The regions identified as significant are anticipated to establish the minimum critical regions harboring genes that contribute to RB tumorigenesis.

Acknowledgments

The authors acknowledge the technical assistance of Courtney MacMullen and Lori Swanson for generation of this data. In addition the assistance of Sharon Diskin, PhD in the initial phase of this study is gratefully acknowledged. This work was supported in part by a grant from NIH/NCI (R21 CA123196-01).

References

1. Lee WH, Bookstein R, Lee EY. Studies on the human retinoblastoma susceptibility gene. J Cell Biochem 1988;38(3):213–27. [PubMed: 3068232]
2. Dyer MA, Bremner R. The search for the retinoblastoma cell of origin. Nat Rev Cancer 2005;5(2):91–101. [PubMed: 15685194]
3. Honavar SG, Singh AD, Shields CL, et al. Postenucleation adjuvant therapy in high-risk retinoblastoma. Arch Ophthalmol 2002;120(7):923–31. [PubMed: 12096963]
4. Makimoto A. Results of treatment of retinoblastoma that has infiltrated the optic nerve, is recurrent, or has metastasized outside the eyeball. Int J Clin Oncol 2004;9(1):7–12. [PubMed: 15162820]
5. Chantada G, Fandino A, Davila MT, et al. Results of a prospective study for the treatment of retinoblastoma. Cancer 2004;100(4):834–42. [PubMed: 14770442]
6. Bowles E, Corson TW, Bayani J, et al. Profiling genomic copy number changes in retinoblastoma beyond loss of RB1. Genes Chromosomes Cancer 2007;46(2):118–29. [PubMed: 17099872]
7. Corson TW, Gallie BL. One hit, two hits, three hits, more? Genomic changes in the development of retinoblastoma. Genes Chromosomes Cancer 2007;46(7):617–34. [PubMed: 17437278]
8. Hong FD, Huang HJ, To H, et al. Structure of the human retinoblastoma gene. Proc Natl Acad Sci U S A 1989;86(14):5502–6. [PubMed: 2748600]
9. Dimaras H, Khetan V, Halliday W, et al. Loss of RB1 induces non-proliferative retinoma: increasing genomic instability correlates with progression to retinoblastoma. Hum Mol Genet 2008;17(10):1363–72. [PubMed: 18211953]
10. Dimaras H, Gallie BL. The p75 NTR neurotrophin receptor is a tumor suppressor in human and murine retinoblastoma development. Int J Cancer 2008;122(9):2023–9. [PubMed: 18196575]
11. Dimaras H, Coburn B, Pajovic S, Gallie BL. Loss of p75 neurotro phin receptor expression accompanies malignant progression to human and murine retinoblastoma. Mol Carcinog 2006;45(5):333–43. [PubMed: 16555252]
12. Windle JJ, Albert DM, O'Brien JM, et al. Retinoblastoma in transgenic mice. Nature 1990;343(6259):665–9. [PubMed: 1689463]
13. Gallie BL, Campbell C, Devlin H, et al. Developmental basis of retinal-specific induction of cancer by RB mutation. Cancer Res 1999;59(7 Suppl):1731s–1735s. [PubMed: 10197588]

14. Chen D, Livne-bar I, Vanderluit JL, et al. Cell-specific effects of RB or RB/p107 loss on retinal development implicate an intrinsically death-resistant cell-of-origin in retinoblastoma. Cancer Cell 2004;5(6):539–51. [PubMed: 15193257]
15. MacPherson D, Sage J, Kim T, et al. Cell type-specific effects of Rb deletion in the murine retina. Genes Dev 2004;18(14):1681–94. [PubMed: 15231717]
16. Dannenberg JH, Schuijff L, Dekker M, et al. Tissue-specific tumor suppressor activity of retinoblastoma gene homologs p107 and p130. Genes Dev 2004;18(23):2952–62. [PubMed: 15574596]
17. Amare Kadam PS, Ghule P, Jose J, et al. Constitutional genomic instability, chromosome aberrations in tumor cells and retinoblastoma. Cancer Genet Cytogenet 2004;150(1):33–43. [PubMed: 15041221]
18. Knudson AG. Hereditary cancer: two hits revisited. J Cancer Res Clin Oncol 1996;122(3):135–40. [PubMed: 8601560]
19. Knudson AG. Two genetic hits (more or less) to cancer. Nat Rev Cancer 2001;1(2):157–62. [PubMed: 11905807]
20. Lillington DM, Kingston JE, Coen PG, et al. Comparative genomic hybridization of 49 primary retinoblastoma tumors identifies chromosomal regions associated with histopathology, progression, and patient outcome. Genes Chromosomes Cancer 2003;36(2):121–8. [PubMed: 12508240]
21. Chen D, Gallie BL, Squire JA. Minimal regions of chromosomal imbalance in retinoblastoma detected by comparative genomic hybridization. Cancer Genet Cytogenet 2001;129(1):57–63. [PubMed: 11520568]
22. Herzog S, Lohmann DR, Buiting K, et al. Marked differences in unilateral isolated retinoblastomas from young and older children studied by comparative genomic hybridization. Hum Genet 2001;108 (2):98–104. [PubMed: 11281459]
23. Mairal A, Pinglier E, Gilbert E, et al. Detection of chromosome imbalances in retinoblastoma by parallel karyotype and CGH analyses. Genes Chromosomes Cancer 2000;28(4):370–9. [PubMed: 10862045]
24. Chow SN, Lin MC, Shen J, et al. Analysis of chromosome abnormalities by comparative genomic hybridization in malignant peripheral primitive neuroectodermal tumor of the ovary. Gynecol Oncol 2004;92(3):752–60. [PubMed: 14984937]
25. Shattuck TM, Kim TS, Costa J, et al. Mutational analyses of RB and BRCA2 as candidate tumour suppressor genes in parathyroid carcinoma. Clin Endocrinol (Oxf) 2003;59(2):180–9. [PubMed: 12864795]
26. Kujawski M, Rydzanicz M, Sarlomo-Rikala M, Szyfter K. Rearrangements involving the 13q chromosome arm committed to the progression of laryngeal squamous cell carcinoma. Cancer Genet Cytogenet 2002;137(1):54–8. [PubMed: 12377414]
27. Hui AB, Pang JC, Ko CW, Ng HK. Detection of chromosomal imbalances in growth hormone-secreting pituitary tumors by comparative genomic hybridization. Hum Pathol 1999;30(9):1019–23. [PubMed: 10492035]
28. Yeager TR, DeVries S, Jarrard DF, et al. Overcoming cellular senescence in human cancer pathogenesis. Genes Dev 1998;12(2):163–74. [PubMed: 9436977]
29. Perry A, Nobori T, Ru N, et al. Detection of p16 gene deletions in gliomas: a comparison of fluorescence in situ hybridization (FISH) versus quantitative PCR. J Neuropathol Exp Neurol 1997;56(9):999–1008. [PubMed: 9291941]
30. Godbout R, Pandita A, Beatty B, et al. Comparative genomic hybridization analysis of Y79 and FISH mapping indicate the amplified human mitochondrial ATP synthase alpha-subunit gene (ATP5A) maps to chromosome 18q12-->q21. Cytogenet Cell Genet 1997;77(3–4):253–6. [PubMed: 9284928]
31. Bayani J, Thorner P, Zielenska M, et al. Application of a simplified comparative genomic hybridization technique to screen for gene amplification in pediatric solid tumors. Pediatr Pathol Lab Med 1995;15(6):831–44. [PubMed: 8705194]
32. Munier FL, Thonney F, Balmer A, et al. Prognostic factors associated with loss of heterozygosity at the RB1 locus in retinoblastoma. Ophthalmic Genet 1997;18(1):7–12. [PubMed: 9134545]

33. Gratias S, Schuler A, Hitpass LK, et al. Genomic gains on chromosome 1q in retinoblastoma: consequences on gene expression and association with clinical manifestation. Int J Cancer 2005;116 (4):555–63. [PubMed: 15825178]
34. Cutler DJ, Zwick ME, Carrasquillo MM, et al. High-throughput variation detection and genotyping using microarrays. Genome Res 2001;11(11):1913–25. [PubMed: 11691856]
35. Li C, Hung Wong W. Model-based analysis of oligonucleotide arrays: model validation, design issues and standard error application. Genome Biol 2001;2(8):RESEARCH0032. [PubMed: 11532216]
36. Lin M, Wei LJ, Sellers WR, et al. dChipSNP: significance curve and clustering of SNP-array-based loss-of-heterozygosity data. Bioinformatics 2004;20(8):1233–40. [PubMed: 14871870]
37. Diskin S, Eck T, Greshock J, Mosse YP, Naylor T, Stoeckert JC, BL Weber, Maris J, Grant G. STAC: A method for testing the significance of DNA copy-number aberrations across multiple array-CGH experiments. Genome Research. 2006In Press
38. Hagstrom SA, Dryja TP. Mitotic recombination map of 13cen-13q14 derived from an investigation of loss of heterozygosity in retinoblastomas. Proc Natl Acad Sci U S A 1999;96(6):2952–7. [PubMed: 10077618]
39. Kawakami M, Staub J, Cliby W, et al. Involvement of H-cadherin (CDH13) on 16q in the region of frequent deletion in ovarian cancer. Int J Oncol 1999;15(4):715–20. [PubMed: 10493953]
40. Zheng L, Lee WH. Retinoblastoma tumor suppressor and genome stability. Adv Cancer Res 2002;85:13–50. [PubMed: 12374284]
41. McCarroll SA, Altshuler DM. Copy-number variation and association studies of human disease. Nat Genet 2007;39(7 Suppl):S37–42. [PubMed: 17597780]
42. Shelling AN, Ferguson LR. Genetic variation in human disease and a new role for copy number variants. Mutat Res 2007;622(1–2):33–41. [PubMed: 17555771]
43. Laurie NA, Donovan SL, Shih CS, et al. Inactivation of the p53 pathway in retinoblastoma. Nature 2006;444(7115):61–6. [PubMed: 17080083]

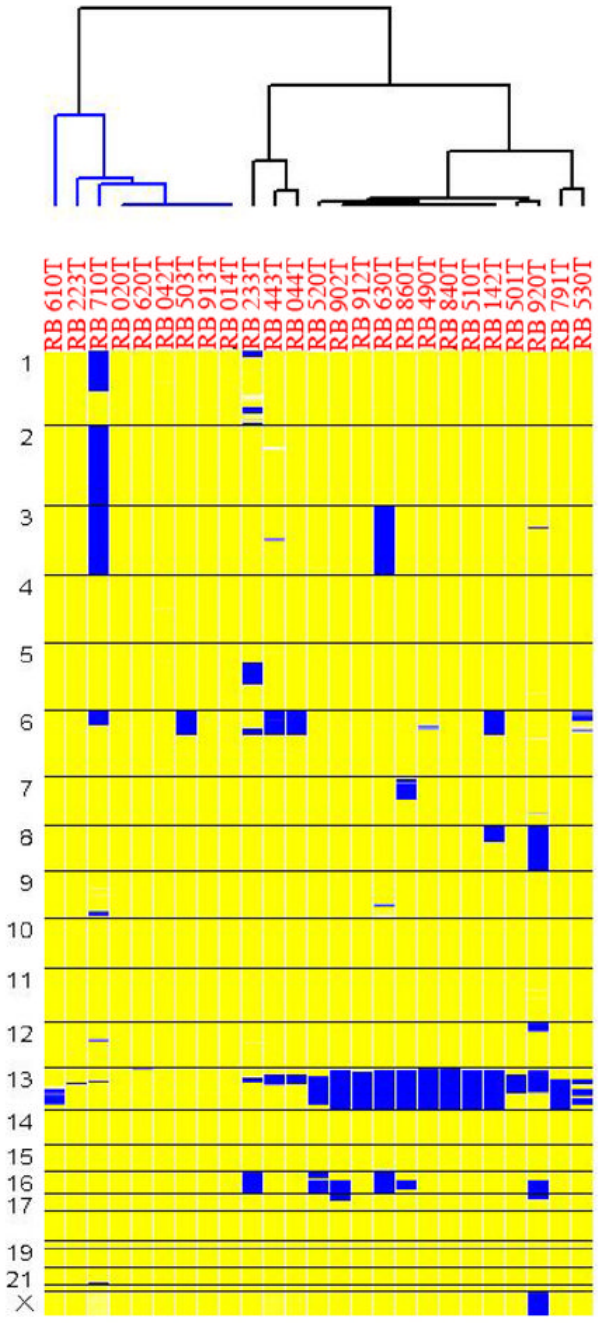

Figure 1.

This picture describes the clustering of 25 RB tumor samples based on their whole genome loss of heterozygosity (LOH) profile. Each column represents a matched normal/tumor pair and each horizontal block indicates a chromosome. The yellow regions indicate retention of heterozygosity (ROH) and blue regions indicate LOH.

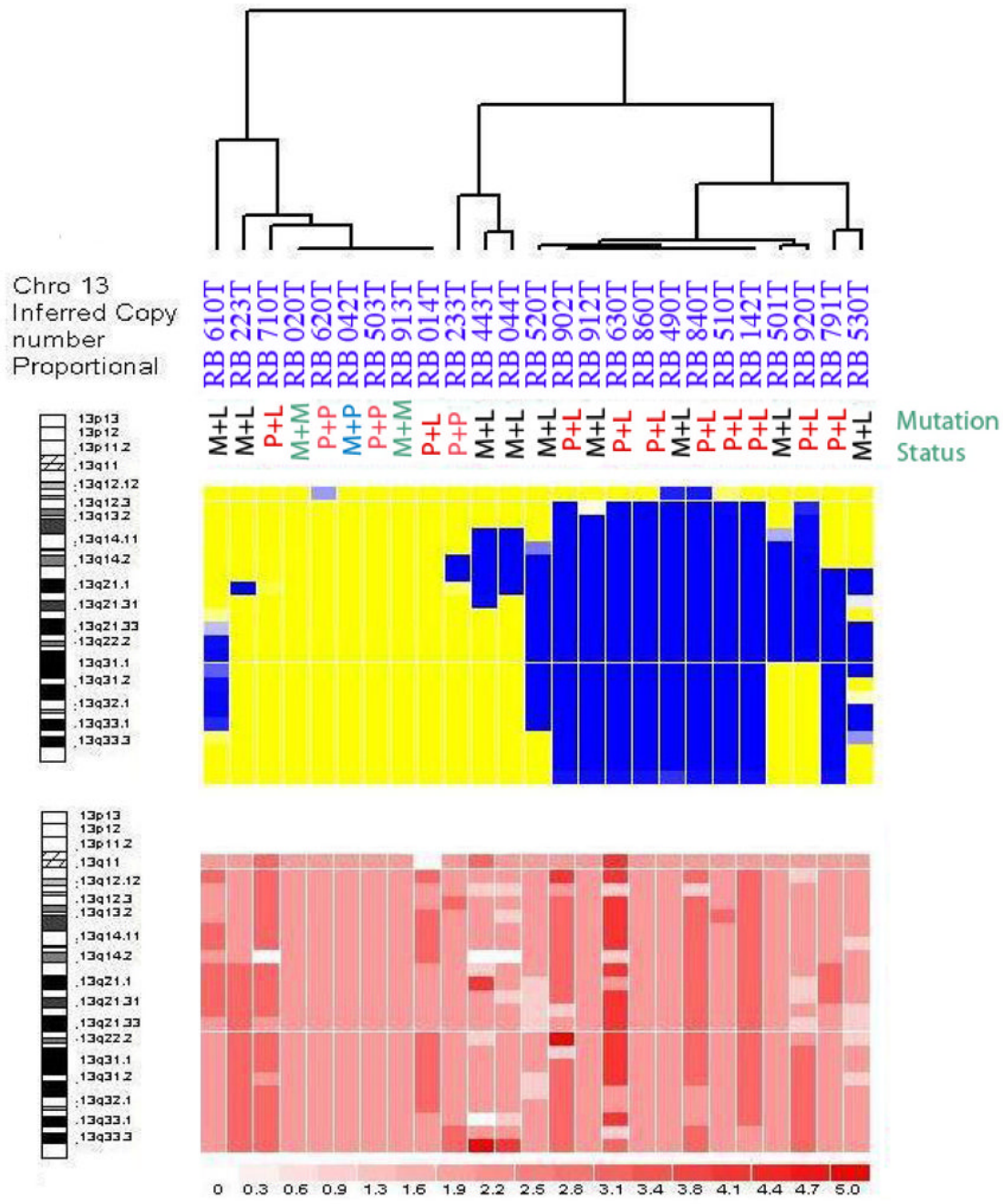

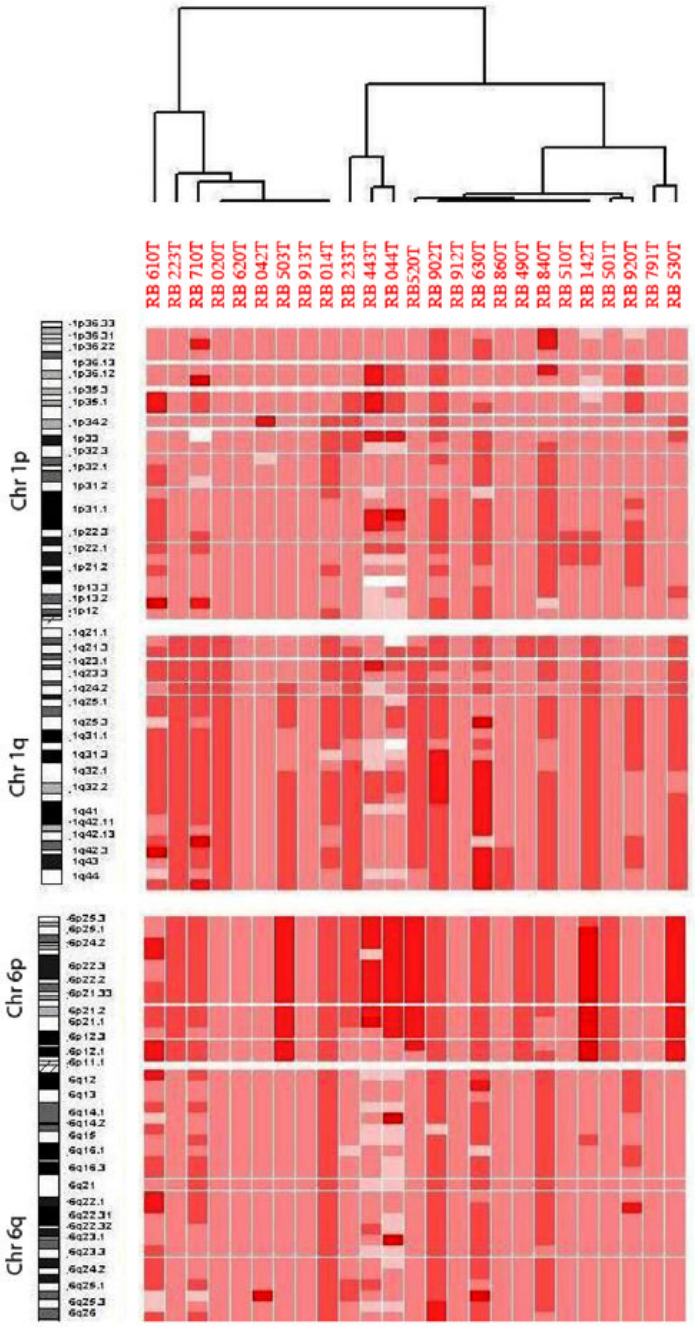

Figure 2.

Figure 2A. This figure represents the results for chromosome 13, which harbors the RB1 gene on 13q14.2 [8].

The different shades of pink indicate different copy numbers white for 0 copy, pink for 2 copies and red for 6 or more copies. The RB tumors cluster according to LOH (upper panel).

Abbreviations: M: Methylation of RB1 promoter; P: Point mutations in the coding sequence of RB1 gene; L: LOH.

Figure 2B. This figure represents chromosomes 1 and 6 aberrations. The amplifications in chromosomes 1q and 6q are correlated. Tumors in the right cluster (12 out of 25) have dark red color for 6p and most likely indicate isochromosome 6p.

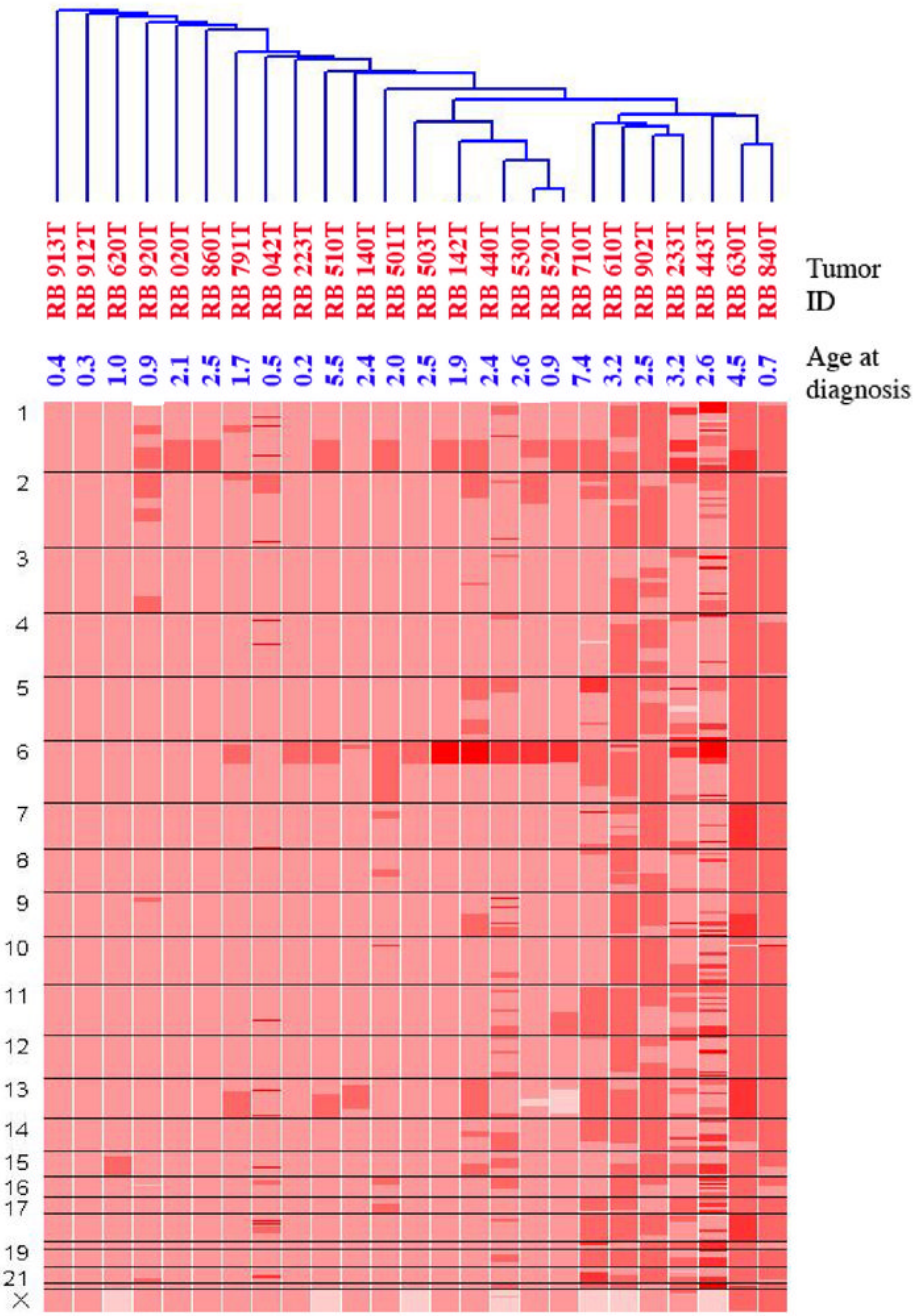

Figure 3.
This figure represents the clustering of RB tumors based on genome wide copy number profiles. The total number of aberrations drives the clustering of tumor subgroups.

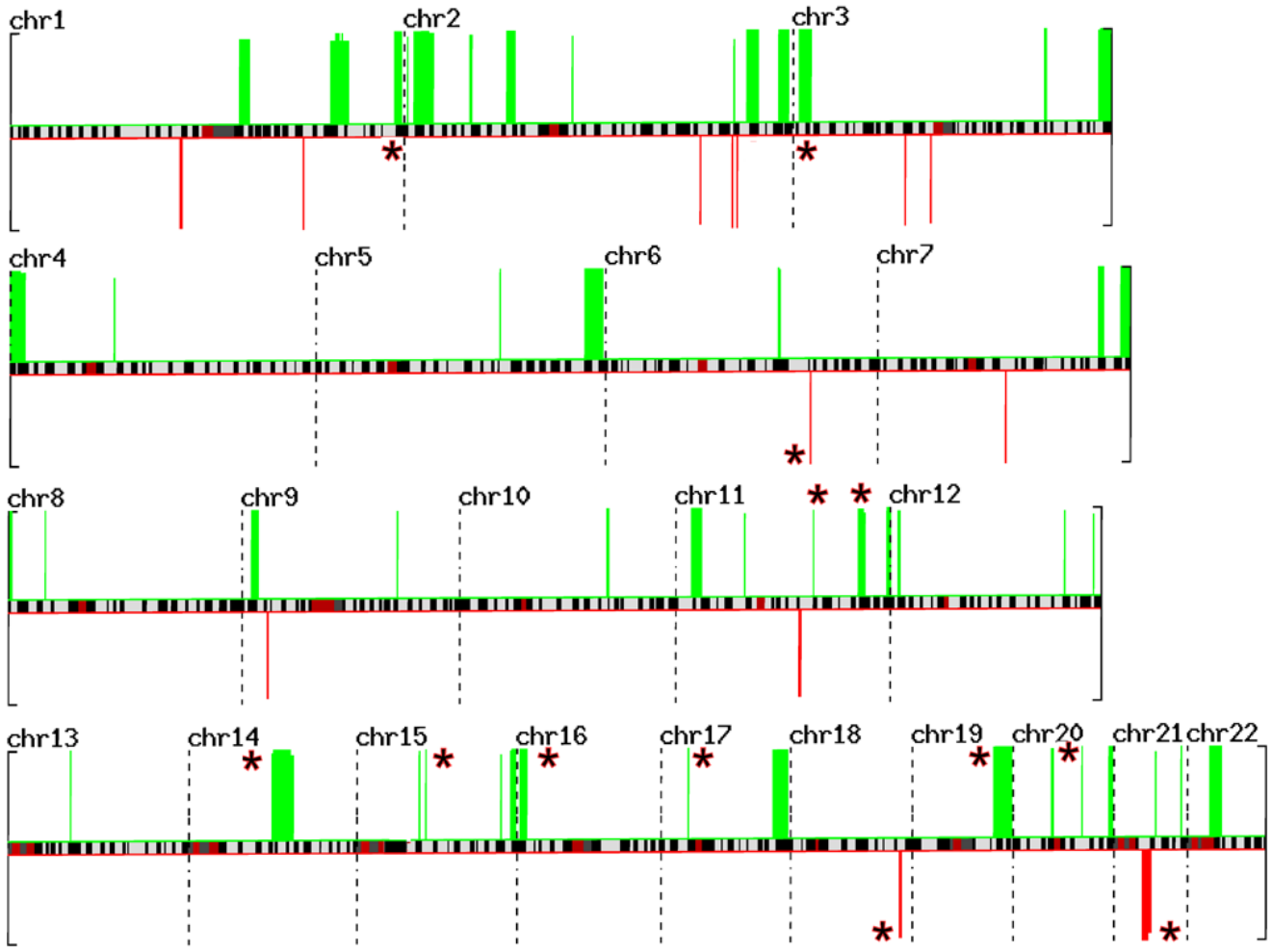

Figure 4.
This figure represents the STAC output for the whole genome displayed across individual chromosomes– the green bars indicate gains and red bars indicate losses. Each bar represents an aberration that has a p-value less than 0.05. The red asterisks indicate 13 novel regions identified in this analysis.

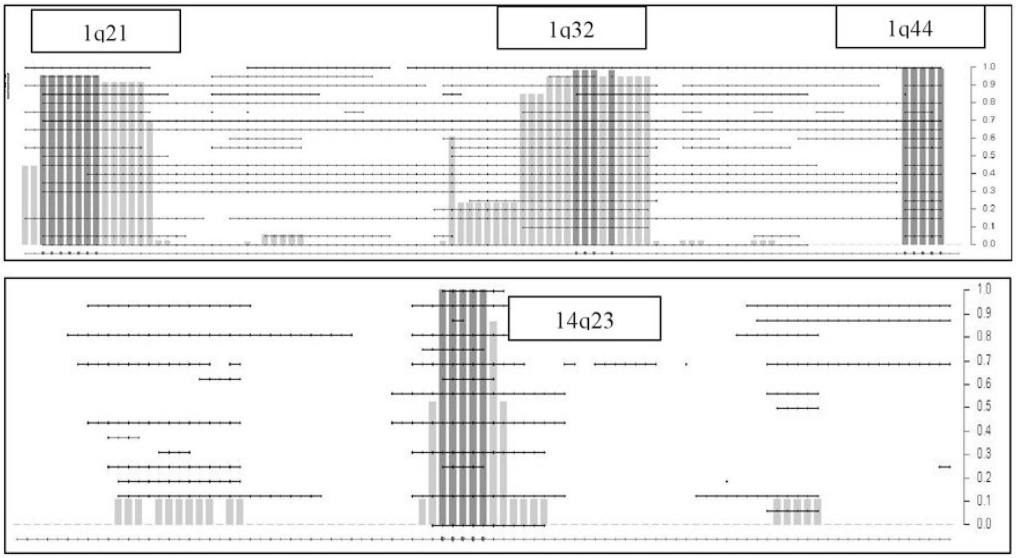

Figure 5.

Figure 5A and 5B. This figure represents the expanded STAC output for chromosomes 1 and 14. The dotted horizontal lines indicate individual tumor profiles. The X-axis included the footprint (fp)-values and Y-axis includes the frequency (f) values.

Table 1

Description of 25 sporadic unilateral RB tumors

ID	Sex	Age at enucleation	LOH of Chromosome 13	Coding Sequence Mutation at RB1 locus	Change (amino acid)/Splicing	Number of Aberrations
014	female	2.0	No	g. 2162C>T, exon 1	p.Q35X	7
020	female	2.1	No	ND*		1
042	female	0.5	No	g. 78238C > T, exon 17	p.R552X	15
044	male	1.1	Yes	ND		25
142	female	2.4	Yes	g. 61797G>A, exon 9	p.G310E	10
223	male	5.5	Yes	ND		3
233	female	3.2	Yes	DEL EXON 15,16 and 20		25
443	male	2.6	Yes	ND		25
490	female	0.2	Yes	ND		1
503	female	1.9	No	g. 76898C>T, exon 15, g. 156833G> A, exon 20	p.R467X, p.W681X	2
501	female	2.4	Yes	g. 76460C> T, exon 14	p.R455X	2
510	male	2.5	Yes	ND		1
520	female	0.9	Yes	ND		5
530	female	0.9	Yes	ND		3
610	male	3.2	Yes	ND		25
620	male	1.0	No	g. 335InsTA, exon 2; g. 2364InsTTGA, exon 22	p.76X, p.750X	1
630	female	4.5	Yes	g. 16184T>A, at −13 position of intron 21	Novel splice acceptor	25
710	male	7.4	Yes	g. 150037C>T, exon 18	p.R579X	16
791	female	1.7	Yes	g. 73750A>G, at −3 position of intron 12.	Novel splice acceptor	4
840	female	0.7	Yes	g. 65386C>T, exon 11	p.R358X,	25
860	female	2.5	Yes	g. 150117 G>A, at +1 position of intron 18	Splice donor	1
902	female	2.5	Yes	g. 160740 G>A, exon 21	p.C706Y	25
912	female	0.3	Yes	ND		0
913	male	0.4	No	ND		0
920	male	0.9	Yes	g. 153198 A> G, at −12 position of intron 18	Novel splice acceptor	5

*ND – Not detected

Table 2

STAC Output for Significant regions of Copy Number Gain in RB Tumors

Chromosomal Gain Regions (based on July 2003 map of UCSC browser)						
arm	**aberration**	**fp (chr)**	**Start (bp)**	**Stop (bp)**	**fp_pvalue**	**fp_confidence (1- fp_pvalue)**
chr1q	Gain	chr1q21.1	143,000,001	150,000,000	0.047952048	0.952047952
chr1q	Gain	chr1q32.1	200,000,001	203,000,000	0.053946054	0.946053946
chr1q	Gain	chr1q32.1	203,000,001	206,000,000	0.01998002	0.98001998
chr1q	Gain	chr1q32.2	206,000,001	207,000,000	0.053946054	0.946053946
chr1q	Gain	chr1q32.3	207,000,001	208,000,000	0.01998002	0.98001998
chr1q	Gain	chr1q32.3	208,000,001	212,000,000	0.053946054	0.946053946
chr1q	**gain**	**chr1q44**	**240,000,001**	**245,000,000**	**0.00999001**	**0.99000999**
chr2p	gain	chr 2p25.3	2,000,001	3,000,000	0.037	0.963
chr2p	gain	chr 2p25.3	6,000,001	16,000,000	0.005	0.995
chr2p	gain	chr 2p24.3	16,000,001	19,000,000	0.018	0.982
chr2p	gain	chr 2p25.3	41,000,001	43,000,000	0.027	0.973
chr2p	gain	chr 2p14	64,000,001	70,000,000	0.005	0.995
chr2q	gain	chr 2q12	105,000,001	106,000,000	0.051948052	0.948051948
chr2q	gain	chr 2q33	206,000,001	207,000,000	0.051948052	0.948051948
chr2q	**gain**	**chr 2q34**	**214,000,001**	**220,000,000**	**0.001998002**	**0.998001998**
chr2q	gain	chr 2q35	220,000,001	222,000,000	0.006993007	0.993006993
chr2q	gain	chr 2q36–37	221,000,001	241,000,000	0.006993007	0.993006993
chr3p	**gain**	**chr3p25.1**	**4,000,001**	**7,000,000**	**0.001998002**	**0.998001998**
chr3p	**gain**	**chr3p25.3**	**9,000,001**	**12,000,000**	**0.001998002**	**0.998001998**
chr3q	**gain**	**chr3p25.31**	**157,000,001**	**159,000,000**	**0.001998002**	**0.998001998**
chr3q	gain	chr3q25	191,000,001	200,000,000	0.01998002	0.98001998
chr4p	gain	chr4p16	1	10,000,000	0.003996004	0.996003996
chr4q	gain	chr4q13.1	65,000,001	66,000,000	0.045954046	0.954045954
chr5q	gain	chr5q23.1	115,000,001	116,000,000	0.005994006	0.994005994
chr5q	gain	chr5q35.2	168,000,001	180,000,000	0.005994006	0.994005994
chr6q	gain	chr6q21	108,000,001	109,000,000	0.007992008	0.992007992
chr6q	gain	chr6q21	109,000,001	110,000,000	0.015984016	0.984015984
chr7q	gain	chr7q34	138,000,001	142,000,000	0.006993007	0.993006993

Chromosomal Gain Regions (based on July 2003 map of UCSC browser)

arm	aberration	fp (chr)	Start (bp)	Stop (bp)	fp_pvalue	fp_confidence (1- fp_pvalue)
chr7q	gain	chr7q36.2-.3	152,000,001	159,000,000	0.002997003	0.997002997
chr8p	gain	chr8p23.3	1,000,001	3,000,000	0.005994006	0.994005994
chr8p	gain	chr8p21.2	23,000,001	24,000,000	0.005994006	0.994005994
chr9p	gain	chr9p24.1-23	6,000,001	11,000,000	0.005994006	0.994005994
chr9q	gain	chr9q31.1	97,000,001	98,000,000	0.016983017	0.983016983
chr10q	gain	chr10q23.31	92,000,001	94,000,000	0.004995005	0.995004995
chr11p	gain	chr11p15	10,000,001	17,000,000	0.005994006	0.994005994
chr11p	gain	chr11p12-11	43,000,001	44,000,000	0.04995005	0.95004995
chr11q	**gain**	**chr11q14.2**	**86,000,001**	**87,000,000**	**0.000999001**	**0.999000999**
chr11q	**gain**	**chr11q23.2-.3**	**114,000,001**	**119,000,000**	**0.000999001**	**0.999000999**
chr11q	**gain**	**chr11q25**	**132,000,001**	**135,000,000**	**0.000999001**	**0.999000999**
chr12p	gain	chr12p13.31	5,000,001	7,000,000	0.026973027	0.973026973
chr12q	gain	chr12q24.11	109,000,001	110,000,000	0.026973027	0.973026973
chr12q	gain	chr12q24.32	127,000,001	128,000,000	0.044955045	0.955044955
chr13q	gain	chr13q14.11	39,000,001	40,000,000	0.005994006	0.994005994
chr14q	**gain**	**chr14q23.1**	**52,000,001**	**64,000,000**	**0.002797202**	**0.997202798**
chr14q	gain	chr14q23.3	64,000,001	66,000,000	0.034965035	0.965034965
chr15q	gain	chr15q15	39,000,001	40,000,000	0.013986014	0.986013986
Arm	**aberration**	**chr**	**Start (bp)**	**Stop (bp)**	**fp_pvalue**	**fp_confidence**
chr15q	**gain**	**chr15q21.1**	**43,000,001**	**44,000,000**	**0.001998002**	**0.998001998**
chr15q	gain	chr15q26.1	90,000,001	91,000,000	0.031968032	0.968031968
chr15q	gain	chr15q26.3	96,000,001	100,000,000	0.013986014	0.986013986
chr16p	**gain**	**chr16p13**	**2,000,001**	**7,000,000**	**0.003996004**	**0.996003996**
chr17p	gain	chr17p11.2	17,000,001	18,000,000	0.002997003	0.997002997
chr17q	gain	chr17q24.3-25.2	70,000,001	80,000,000	0.015984016	0.984015984
chr19q	**gain**	**chr19q13.3**	**51,000,001**	**63,000,000**	**0.003996004**	**0.996003996**
chr20p	gain	chr 20p11.21	24,000,001	26,000,000	0.015984016	0.984015984
chr20q	**gain**	**chr 20q13.12**	**43,000,001**	**44,000,000**	**0.000999001**	**0.999000999**
chr20q	**gain**	**chr 20q13.33**	**60,000,001**	**63,000,000**	**0.000999001**	**0.999000999**
chr21q	gain	chr 21q21.3	26,000,001	27,000,000	0.03996004	0.96003996

Chromosomal Gain Regions (based on July 2003 map of UCSC browser)						
arm	**aberration**	**fp (chr)**	**Start (bp)**	**Stop (bp)**	**fp_pvalue**	**fp_confidence (1- fp_pvalue)**
chr21q	**gain**	**chr 21q22.3**	**42,000,001**	**43,000,000**	**0.003996004**	**0.996003996**
chr22q	gain	chr 22q11.1-.22	14,000,001	22,000,000	0.008991009	0.991008991
			Chromosomal Loss Regions			
chr1p	loss	chr1p21.1-13.3	106,000,001	108,000,000	0.017982018	0.982017982
chr1q	loss	chr1q31.1	183,000,001	184,000,000	0.005994006	0.994005994
chr2q	loss	chr 2q32.1	185,000,001	186,000,000	0.024975025	0.975024975
chr2q	loss	chr 2q33.1	205,000,001	206,000,000	0.001998002	0.998001998
chr2q	loss	chr 2q33.3	208,000,001	209,000,000	0.001998002	0.998001998
chr3p	loss	chr3p13	70,000,001	71,000,000	0.010989011	0.989010989
chr3p	loss	chr3p12.1	86,000,001	87,000,000	0.024975025	0.975024975
chr6q	**loss**	**chr6q22.33**	**128,000,001**	**129,000,000**	**0.000999001**	**0.999000999**
chr7q	**loss**	**chr7q21.11**	**80,000,001**	**81,000,000**	**0.002997003**	**0.997002997**
chr9p	loss	chr9p22.3-22.2	16,000,001	17,000,000	0.032967033	0.967032967
chr11q	loss	chr11q13.5-14.1	77,000,001	79,000,000	0.034965035	0.965034965
chr18q	loss	chr18q22.2	68,000,001	70,000,000	0.021978022	0.978021978
chr21q	**loss**	**chr 21q21.1**	**18,000,001**	**22,000,000**	**0.00999001**	**0.99000999**
chr21q	loss	chr 21q21.1	22,000,001	24,000,000	0.047952048	0.952047952